AD-A275 274

REPORT DOCUMENTATION PAGE

Form Approved OMB No. 0704-0188

1. AGENCY USE ONLY

3. REPORT TYPE AND DATES COVERED
THESIS/DISSERTATION

4. TITLE AND SUBTITLE
Determination of Pressure Response Times for Gaseous Flow in a Tube

5. FUNDING NUMBERS

6. AUTHOR(S)
Scott A. Baune

7. PERFORMING ORGANIZATION NAME(S) AND ADDRESS(ES)
AFIT Student Attending: Joint Inst Advance of Flight Sciences

8. PERFORMING ORGANIZATION REPORT NUMBER
AFIT/CI/CIA-93-1170

9. SPONSORING/MONITORING AGENCY NAME(S) AND ADDRESS(ES)
DEPARTMENT OF THE AIR FORCE
AFIT/CI
2950 P STREET
WRIGHT-PATTERSON AFB OH 45433-7765

10. SPONSORING/MONITORING AGENCY REPORT NUMBER

DTIC ELECTE FEB 02 1994 S E D

11. SUPPLEMENTARY NOTES

12a. DISTRIBUTION/AVAILABILITY STATEMENT
Approved for Public Release IAW 190-1
Distribution Unlimited
MICHAEL M. BRICKER, SMSgt, USAF
Chief Administration

12b. DISTRIBUTION CODE

13. ABSTRACT (Maximum 200 words)

DTIC QUALITY INSPECTED 2

Accesion For	
NTIS CRA&I	X
DTIC TAB	☐
Unannounced	☐
Justification	
By	
Distribution /	
Availability Codes	
Dist	Avail and / or Special
A-1	

14. SUBJECT TERMS

15. NUMBER OF PAGES
100

16. PRICE CODE

17. SECURITY CLASSIFICATION OF REPORT

18. SECURITY CLASSIFICATION OF THIS PAGE

19. SECURITY CLASSIFICATION OF ABSTRACT

20. LIMITATION OF ABSTRACT

NSN 7540-01-280-5500

Standard Form 298 (Rev. 2-89)
Prescribed by ANSI Std. Z39-18
298-102

2nd Jl

Baune

93-1170

SCOTT A. BAUNE

Determination of Pressure Response Times for Gaseous Flow in a Tube

The motivation for determining the response time for a pressure regulator to adjust the pressure at an area of interest located at the end of a long tube may be due to several reasons. One of these is the possibility that the regulator cannot be conveniently controlled from a more desirable position closer to the area of interest. Another reason to place the regulator a long distance from the area of interest might be to avoid high pressure lines over a prolonged distance. Consider the system shown in Figure 1, which is the proposed propulsion system for a microgravity experiment located in the Shuttle cargo bay. The regulator is controlled electronically so the ability to reduce the amount of electrical wiring will increase system reliability. Furthermore, Shuttle safety requirements demand that high pressure lines be tested for space worthiness, thus placement of the regulator close to the propellant source may eliminate the presence of these high pressure lines.

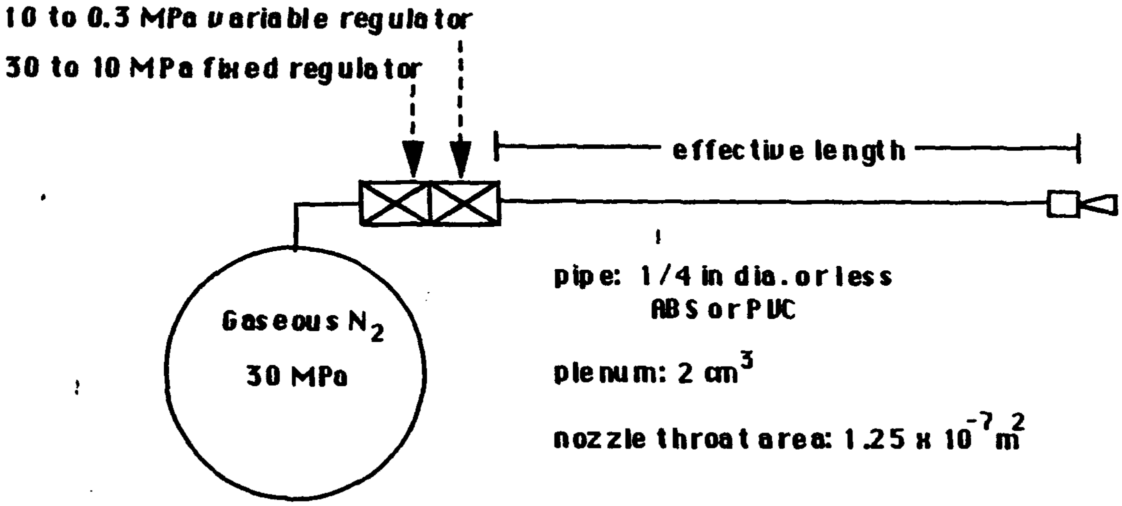

Figure 1: Proposed Microgravity Propulsion System

To determine the time delay for the system above, it is assumed that the pressure loss due to gas escaping out the nozzle throat area is negligible and that the initial start-up delay will be the longest delay encountered. The latter assumption is valid when one considers that the pressure in the tube and plenum are essentially zero before the regulator is activated. For a worst case scenario, we will assume that the first command to the regulator will demand the maximum pressure of 10 MPa.

Given a demand of 10 MPa in the plenum, the first step in this pneumatics problem is to determine the effective pipe length and pressure loss in the system. Assuming 30 ft of ABS (thermoplastic polymer) or PVC pipe is used and that four 90° elbow joints are needed, the effective pipe length may be found from:

$$L_{eff} = L_{st} + nCFD^{1.2}$$

where L_{st} is the length of straight pipe, n is the number of joints, C is a constant equal to 43.7 for length in feet and diameter in inches, F is the resistance coefficient of the fittings used (0.5 for 90° elbow joints), and D is the pipe diameter.[1] For the system shown, the pipe diameter will be 1/4 inch or less.

The pressure loss associated with a given effective length is found from:

$$\Delta P = FLQ \,/\, PD^{5.33}$$

where ΔP is the pressure loss in bars, F is a friction factor (500 for steel pipe, variable for ABS or PVC pipe), L is the effective length, Q is the flow rate, P is the final pressure (10 MPa, or 100 bar), and D is the pipe diameter in mm.[1] These figures result in a calculated pressure loss of about 3 bar (0.3 MPa), or only 3% of the desired pressure, for a pipe diameter of 1/4 in (6.35 mm) and a flow of 27.43 liters/sec. As a result, it is safe to assume negligible pressure loss.

Having determined the effective pipe length and pressure loss, the delay time for the pipe and plenum to pressurize to the desired 10 MPa may be determined. Assuming that the gaseous nitrogen acts as a perfect gas, and that conservation of mass momentum, and energy hold, we may use the following set of coupled equations:[2]

Perfect Gas Law: $$P = \rho R T$$

Momentum Equation: $$\rho\left[\frac{dv}{dt} + v\frac{dv}{dx}\right] + \frac{dP}{dx} = 0$$

Continuity Equation: $$A(x)\frac{d\rho}{dt} + \frac{d}{dx}(\rho A v) = 0$$

Energy Equation: $$\rho\frac{d}{dt}\left(E + \frac{1}{2}v^2\right) + \frac{d}{dx}\left[\rho\left(E + \frac{1}{2}v^2\right)v + Pv\right] = 0$$

where P is pressure, ρ is density, R is the gas constant for GN_2 (296.7972 m^2/s^2K^o), T is absolute temperature, v is the gas velocity, A is the pipe cross sectional area, E is the product of the specific volume and temperature, and x is the location down the pipe (x = 0 at the regulator, x = L at the plenum). Assuming the temperature of the gas remains constant at -20°C (253.15 °K), the energy term (C_vT) remains constant. As a result, the energy derivatives are zero and the associated equation reduces to the momentum equation leaving three equations and three unknowns (P, ρ, v). These equations, however, are coupled, presenting a nontrivial problem when solved analytically. For simplicity, then, a numerical solution to this set of equations will be sought, assuming the errors involved are acceptable.

Given that the regulator valve opening time may be considered instantaneous (*typical valve opening times are around 0.01 to 0.03 sec.*), we may assume that the effective pipe cross sectional area is a constant, so the force acting on the gas is also a constant ($F = PA$). Given this assumption, the time for Poiseuille flow to form within the pipe may be found. This flow represents the parabolic flow of a fluid or gas in a pipe due to a pressure gradient. Once Poiseuille flow has formed, the fluid traveling along the centerline of the pipe is at a maximum velocity for the given pressure differential. For starting flow in a pipe, it may be assumed that the time for Poiseuille flow to form is given by:[2]

$$t = 0.75 r^2 \rho / \mu$$

where r is the pipe radius, ρ is the gas density, and μ is the gas viscosity. Given that GN_2 at 10 MPa and -20°C has a density of 154 kg/m^3 and a viscosity of 14.826 kg/m sec^{-1}, the Poiseuille flow in a 1/4 inch diameter pipe occurs in 8×10^{-5} sec, which may be assumed to be instantaneous.

Given that the development of Poiseuille flow will not cause a significant time delay, the time for the pipe and plenum to pressurize may be found by determining the mass flow rate of the gas and the associated rate of pressure change. Next, performing numerical integration by taking infinitesimally small time steps, the pressure in the pipe and plenum may be found. Finally, this pressure is used to determine a new mass flow rate and the process is continued until the desired pressure is achieved.

Four assumptions associated with this process are: 1) the pipe has some very small initial pressure, 2) the change in pressure within the pipe and plenum is uniform down the entire pipe and plenum length, 3) the friction loss in the pipe is negligible due to the earlier calculation of the effective length, and 4)

the change in fluid velocity over each time step (dv/dt) is zero.

Determining the mass flow rate involves dividing the momentum equation by ρv^2 and replacing ρ with P/RT and v^2 with $(\dot{m}/A\rho)^2$ to yield:

$$\frac{PA^2}{\dot{m}^2 RT} dP + \frac{1}{\upsilon} d\upsilon = 0$$

integrating each term yields:

$$P_{reg}^2 - P^2 = \frac{2\dot{m}^2 RT}{A^2} \ln\left[\frac{P_{reg}}{P}\right]$$

solving for the mass flow rate:

$$\dot{m} = \sqrt{\left(P_{reg}^2 - P^2\right)\frac{A^2}{2RT \ln\left[\frac{P_{reg}}{P}\right]}}$$

where P_{reg} is the pressure leaving the regulator (10 MPa), P is the pipe and plenum pressure and is initially not zero, and A, R, and T are as previously defined.

Differentiating the perfect gas law and replacing the density with the fluid mass/pipe and plenum volume (V), produces:

$$\dot{P} = \dot{m}RT/\upsilon$$

Having determined the rate of pressure change for the given time step, the pipe and plenum pressure may now be found from a simple Euler equation:

$$P_{new} = P_{old} + \dot{P}dt$$

Finally, updating the time so t = t + dt completes the cycle. Repeating this pattern over infinitesimally small time steps until $P = P_{reg}$ will yield the time to

pressurize the pipe and plenum. Using this approach, the time to pressurize the system from 0 to 10 MPa for various pipe diameters is shown in Figure 2.

Once the system has been pressurized to 10 MPa, the next concern may be the time delay involved in reducing the system pressure, as opposed to building it up. For the particular system shown in Figure 1, the only way to reduce the pressure is by lowering the pressure output from the regulator and letting gas bleed from the nozzle. A modification to the system might include a relief T-valve on the system to vent the excess gas. Although this would cause a discontinuity in microgravity acceleration measurements, the pressure reduction would be nearly instantaneous. To determine the bleed-down time associated with just the nozzle, the same numerical integration approach used earlier applies. One major difference, however, is the mass flow rate equation is for a supersonic nozzle and is a function of the throat area:[3]

$$\dot{m} = A_t P k \sqrt{\frac{\left(2/(k+1)\right)^{(k+1)/(k-1)}}{kRT}}$$

where k is the ratio of specific heats which, for nitrogen operating in a pressure range of 0.3 to 10 MPa at -20°C, is 1.432 to 1.783. Also, the updated pressure is $P_{new} = P_{old} - \dot{P}dt$. Figure 3 shows the time delay for the system to bleed from 10 to 0.3 MPa given various pipe diameters.

In conclusion, a numerical solution to determine the time delay associated with pressurizing an area of interest due to placing the pressure regulator upstream from that area has been presented. Although several assumptions have been made, by taking a worst case scenario approach the resulting solution should yield a rough idea of the anticipated time delay.

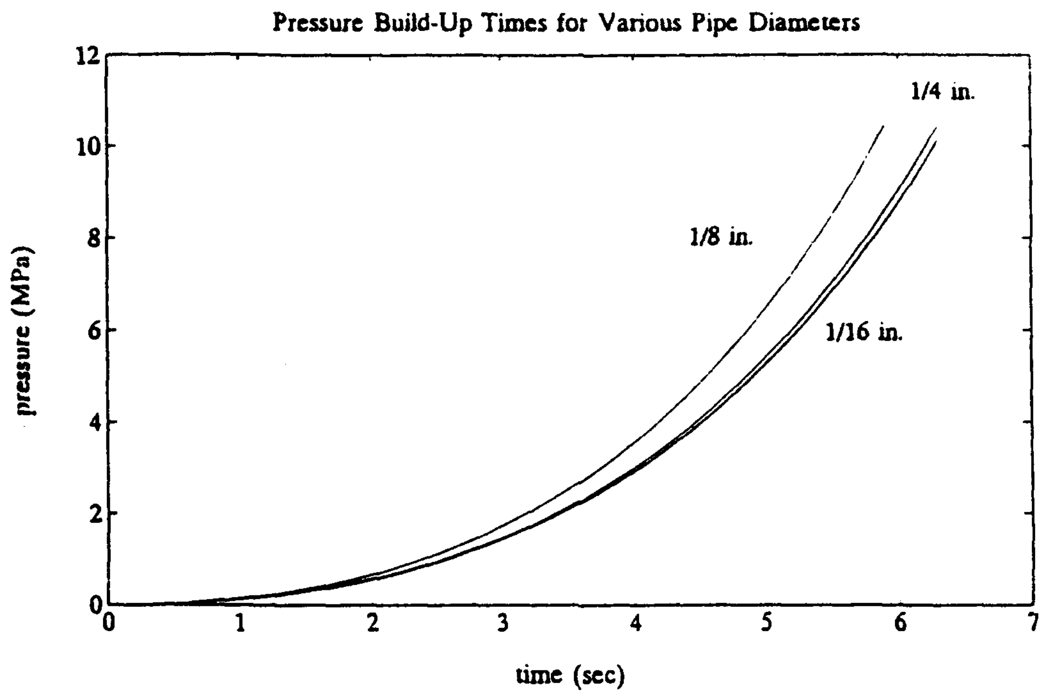

Figure 2

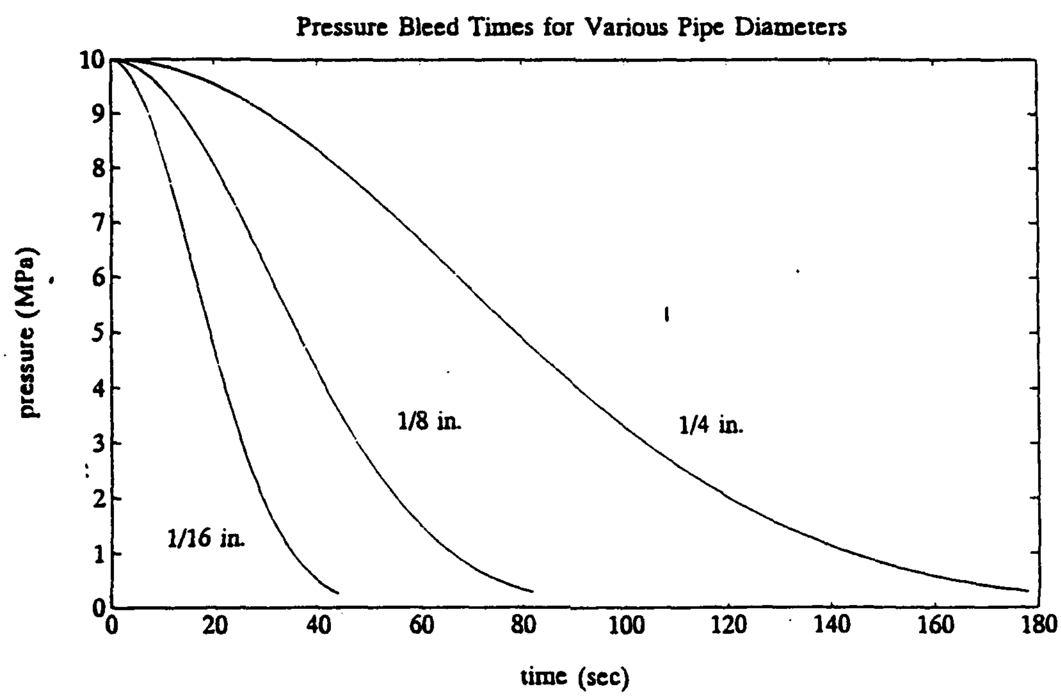

Figure 3

References

1. *Warring, R.H. <u>Pneumatic Handbook.</u> 6th ed. Gulf Publishing, Houston, 1982. Pp 146-155.*

2. *White, Frank M. <u>Viscous Fluid Flow.</u> Mcgraw-Hill, 1974. Pp 112, 140-145, 661.*

3. *Sutton, George P. <u>Rocket Propulsion Elements.</u> 5th ed. Wiley & Sons, New York, 1986. Pp 46.*

Determination of Shuttle Limit Cycles for Various Angles of Attack and Deadbands

by Scott Baune

The purpose of this paper is to analytically determine the limit cycle of the shuttle about the pitch axis for various angles of attack and deadbands. The angle of attack, α, is defined by the rotation about the shuttle y-axis so that $\alpha = 90^o$ is gravity gradient stable. The deadband is the region of deviation from α that the shuttle will be allowed to drift before corrections are implemented by the Reaction Control System (RCS). Therefore, an α of 50^o with a deadband of $\pm 5^o$ would allow the shuttle to drift from $\alpha_l = 45^o$ up to $\alpha_h = 55^o$ without RCS control.

The primary source of disturbance about the pitch axis above an altitude of 200 km is assumed to be the gravity gradient torque given by:

$$P_{max} \sin 2\alpha$$

where P_{max} is defined as the maximum gravity gradient torque for a given altitude. This torque occurs at $\alpha=\pi/4$ and is given by:

$$P_{max} = \frac{3GMe}{2(h+Re)^3} (I_{xx} - I_{zz})$$

where $GM_e = 398{,}601.2\ km^3/s^2$, $R_e = 6378.137$ km, $I_{xx} = 1{,}340{,}000\ Nms^2$, $I_{zz} = 10{,}200{,}000\ Nms^2$, and h is the orbital altitude.

To determine the limit cycle due to gravity gradient, the moments acting about the pitch axis are summed as:

$$\Sigma M = I_{yy} (d^2\alpha/dt^2) = P_{max} \sin 2\alpha$$

where I_{yy} = 9,910,000 Nms^2. It should be noted that the given moment of inertia values are typical but will vary from mission to mission.

At this point the notation shown in Figure One is implemented so that $ø + \alpha = 90^o$ and $(d^2\alpha/dt^2) = -(d^2ø/dt^2)$.

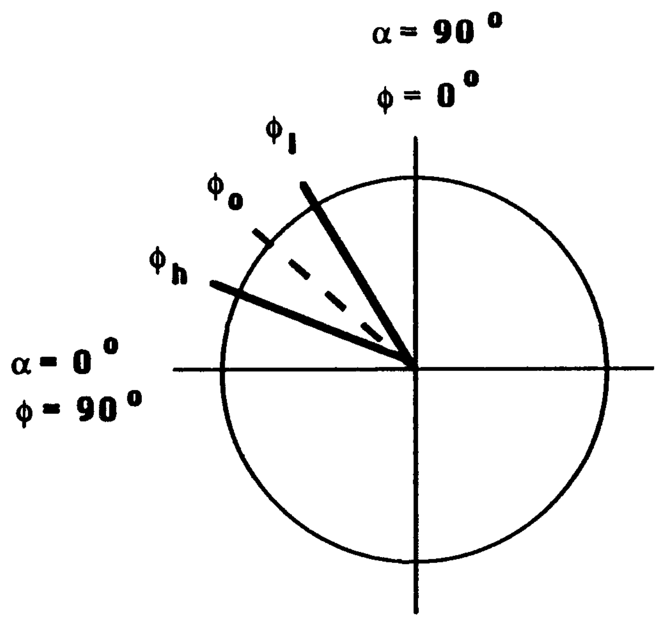

Figure One: Angle Notation

As a result of this change, the moment equation may now be written as:

$$\Sigma M = I_{yy} (d^2ø/dt^2) = -P_{max} \sin 2ø$$

Integration of this equation produces:

$$(d\phi/dt)^2 = (P_{max}/I_{yy}) \cos 2\phi + C$$

where C is a constant of integration found from the initial conditions that $d\phi/dt$ and ϕ at $t = 0$ are 0 rad/sec and ϕ_h, respectively. Therefore, substitution of C and implementation of $\cos 2\phi = 1 - 2\sin 2\phi$ yields:

$$(d\phi/dt)^2 = 2(P_{max}/I_{yy}) \sin 2\phi_h \, (1 - n^2 \sin 2\phi)$$

where $n = 1/\sin\phi_h$.

Solving for the time to drift from some angle ϕ to gravity gradient stable ($\alpha = 90^\circ$ and $\phi = 0^\circ$) yields:

$$t = \frac{1}{\sqrt{2 \dfrac{P_{max}}{I_{yy}} \sin 2\phi_h}} \int_0^{\phi} \frac{d\phi}{\sqrt{1 - n^2 \sin 2\phi}}$$

By definition, the elliptic integral above may be stated as:

$$t = kc \, F(\beta, k)$$

where k is known as the modulus and is given by $1/n$, or $\sin\phi_h$, c is the constant term in front of the integral above, and $F(\beta,k)$ is the value of the elliptic integral easily found in tabulated form or computationally with β given by:

$$\sin\beta_{h,l} = n \sin\phi_{h,l}$$

To determine the total drift time, T, across a region from ϕ_l, through ϕ_h, and back to ϕ_l as shown in Figure Two, the time difference between these two integrals must be found, then doubled. The time is doubled because the difference between the two integrals from ϕ_h to ϕ_l only accounts for the upper half of the curve in Figure Two based on the given initial conditions. Thus the total drift time is given by:

$$T = 2kc \{F(\beta_h,k) - F(\beta_l,k)\}$$

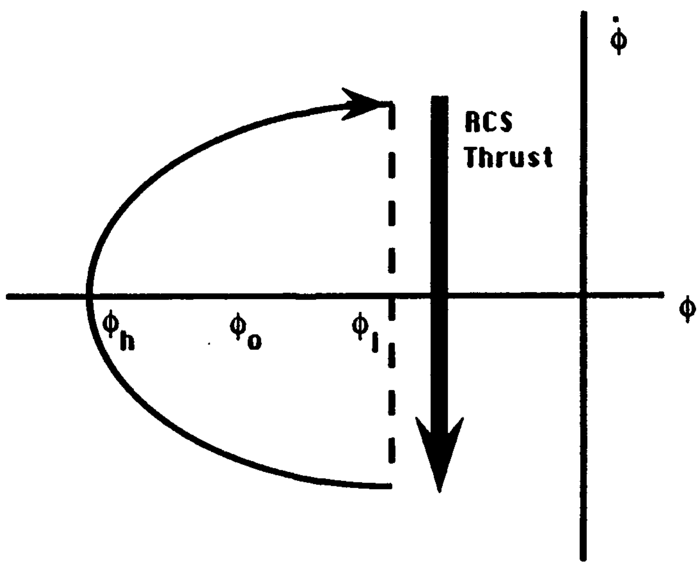

Figure Two: Limit Cycle Curve

As shown, Figure Two illustrates the the drift rate of the shuttle about the pitch axis versus the pitch angle. The initial conditions, that is, $d\phi/dt = 0$ rad/sec and $\phi = \phi_h$ at $t = 0$, used in the elliptic integral formulation may then be seen at the left portion of the curve, as well as the pitch rate at the end condition, ϕ_l. Finally, returning to the the lower position on Figue Two requires the use of RCS thrusters and is considered instantaneous in the formulation above. However, if the force of the thrust, F, and the distance from the shuttle center of gravity, D, are known, the thrust duration may be found from:

$$t = (2I_{yy}/FD)\ d\phi/dt$$

Implementation of this derivation was accomplished using an altitude of 275 km, where $P_{max} = 18$ nm. Figure Three shows the drift time in minutes for various angles of attack and deadbands of ± 2, 3, 4, 5, and 10°.

To check the results of this graph, a new formulation which holds the gravity gradient torque constant at its maximum level, despite changes in α, was made so that:

$$\phi(t) = -\{\ (P_{max}/2I_{yy})\ \sin 2\phi\ \}\ t^2 + \phi_h$$

and the total drift time, T, is given by:

$$T = 2t = \sqrt{\frac{\phi_h - \phi_l}{\frac{P_{max}}{2I_{yy}} \sin 2\phi}}$$

Figure Four compares the results of the fixed torque formulation to Figure Three for deadbands of ± 2 and 10°. This comparison reveals similiar results

around the $\alpha = 45^o$ area but not around the ends. These results appear reasonable since the gravity gradient torque at 45^o is the same for the fixed torque case and the elliptic integral case, but as α approaches 0 or 90^o, the gravity gradient torque reduces to zero in the elliptic integral case, while remaining constant in the fixed torque case.

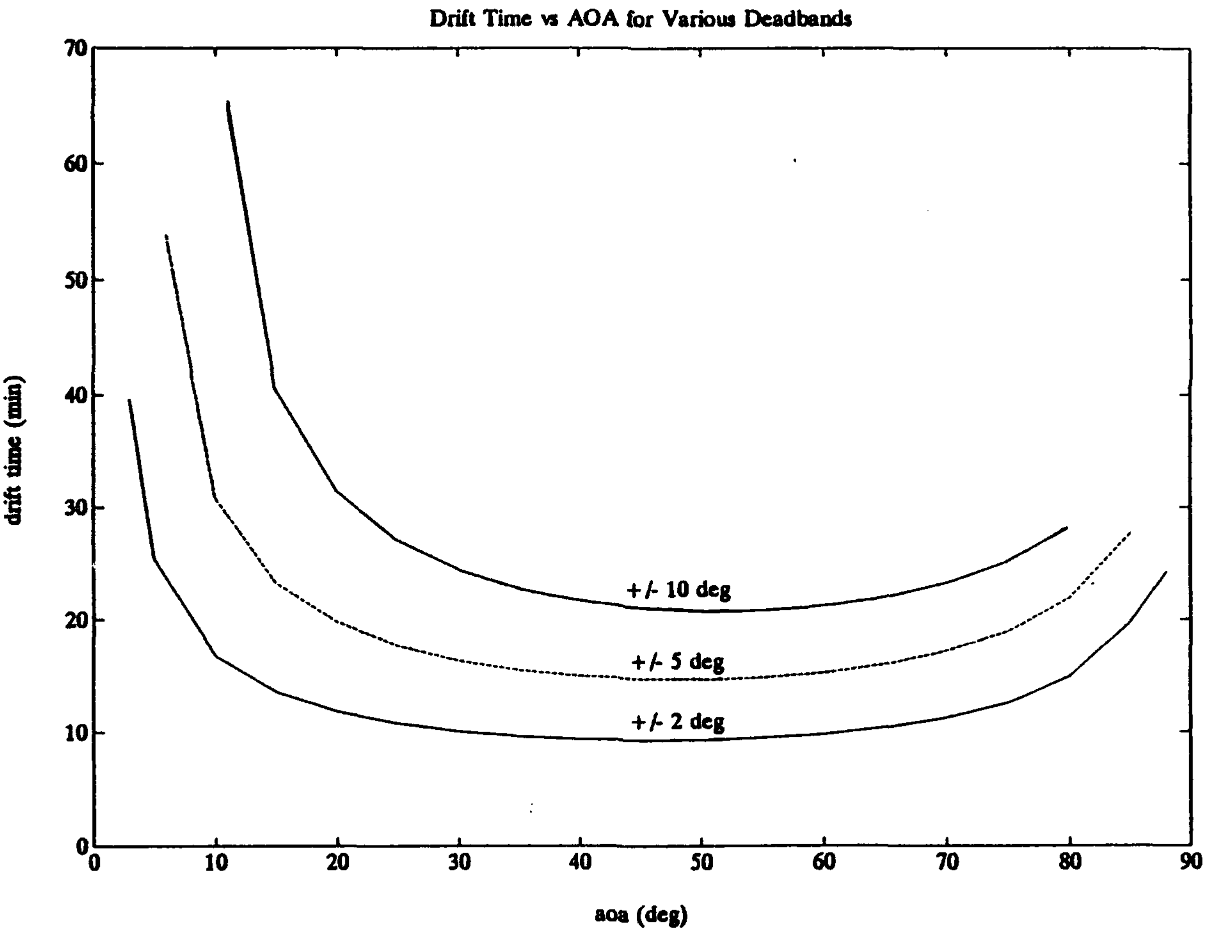

Figure Three

Drift Time vs. AOA for
+/- 10 degree deadband

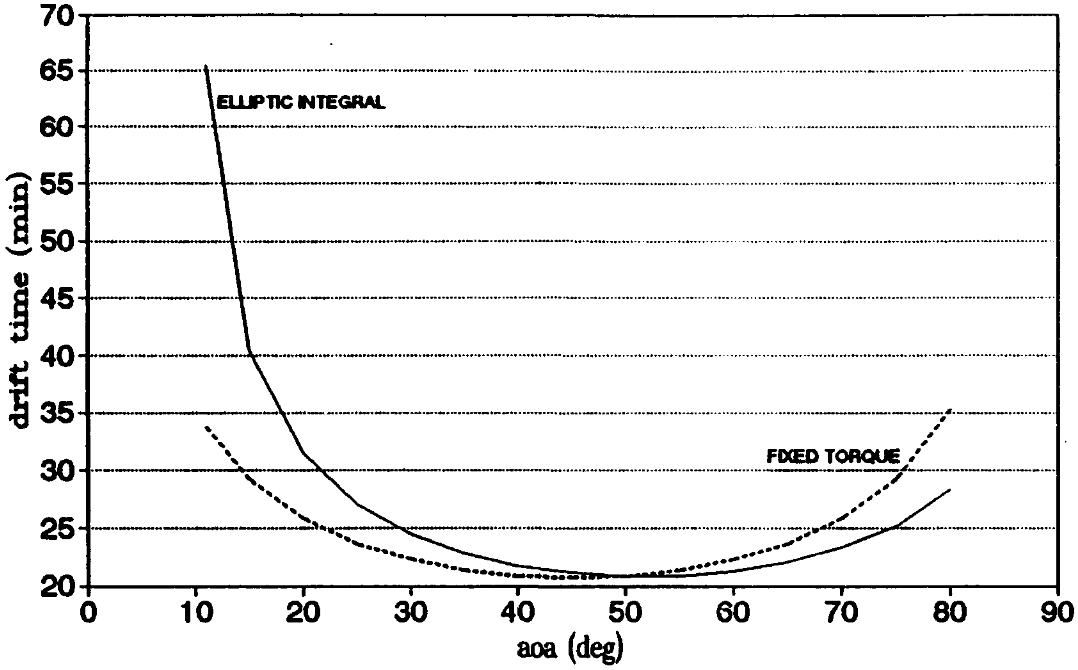

Drift Time vs AOA for
+/- 2 degree deadband

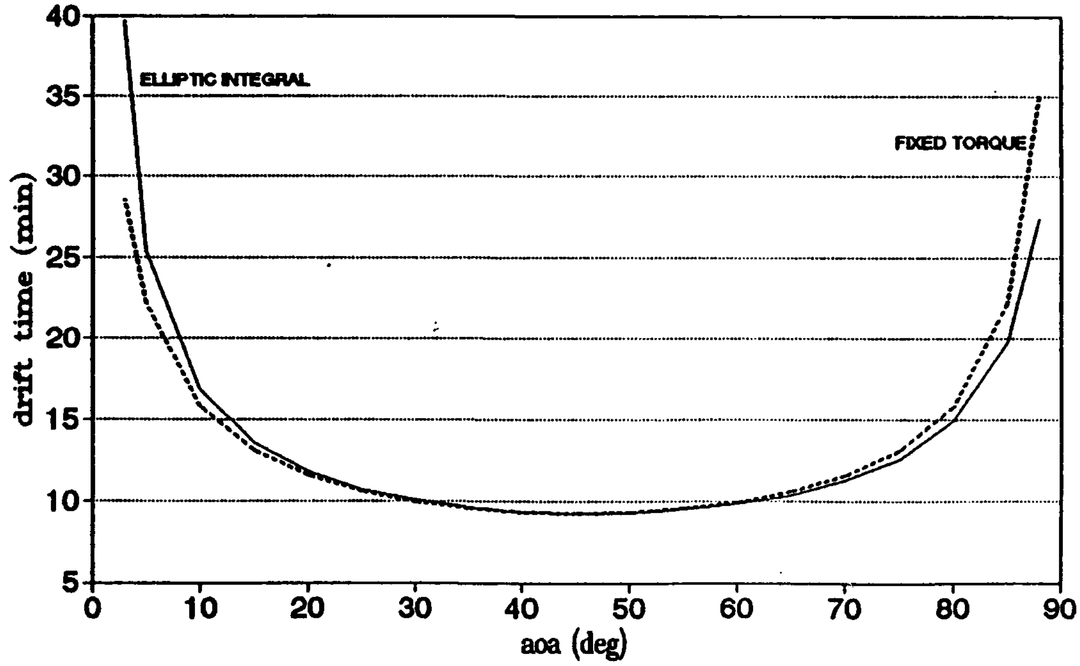

FIGURE FOUR

References

Byrd P.F. and M.D. Friedman Handbook of Elliptic Integrals for Engineers and Scientists. 2nd ed. Springer-Verlag: Berlin, 1971.

SCOTT A. BAUNE

Design of a Variable Thrust Cold Gas Microthruster Nozzle

The motivation for the design of a variable thrust microthruster stems from the desire to counter the gravity gradient and drag accelerations present on a microgravity facility or experiment located at positions other than the center of gravity of another facility (i.e. the Shuttle or Space Station). Research in the development of microthrusters began as early as the 1950's with the development of hot gas thrusters. These thrusters were scaled versions of larger variable thrust engines which had already been developed. Failure of these thrusters was mainly a result of materials failure caused by the combustion of the propellant. Recently, however, microthrusters using a cold gas propellant such as nitrogen or ammonia have been developed for attitude control and microgravity research.

These systems incorporate a regulator to vary the pressure of the gas inside a collection chamber. The gas then passes through a nozzle *via* a constricted region known as the throat, producing thrust at the nozzle exit. The design of the nozzle for a cold gas consists of determining certain critical parameters shown in Figure 1. These include throat area, A_t, chamber pressure, P_1, chamber temperature, T_1, divergence angle, α, and expansion ratio, A_2/A_t.

Assuming that isentropic relations hold inside the chamber and nozzle generally allows us to calculate performance to within 10% of the measured values. As a result, the design process illustrated here is limited to this ideal rocket case. Once the ideal rocket analysis is complete, the results must be corrected to account for the following actual conditions present within the engine:[1]

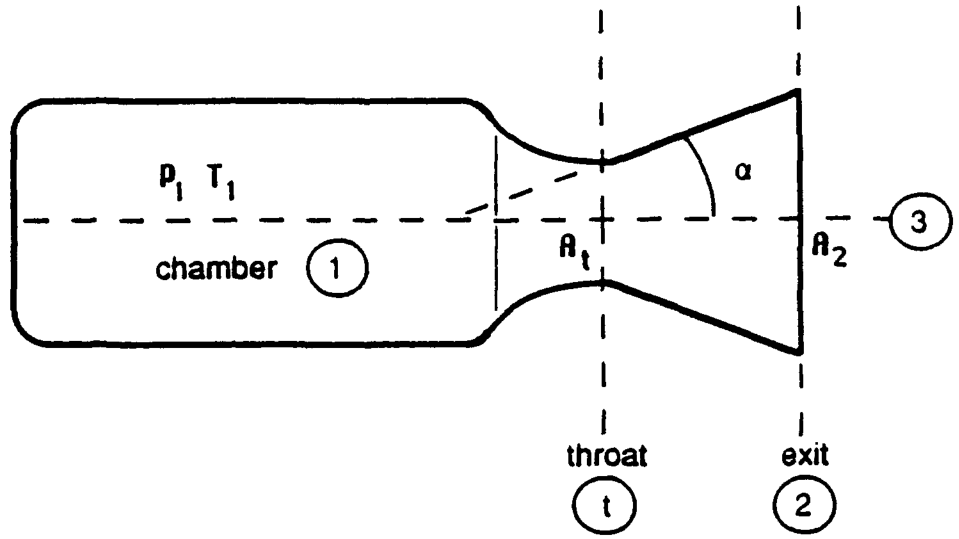

Figure 1: Thrustor notation and Critical Parameters

1. Conical divergence of the exhaust jet.
2. Surface friction and flow disturbances in the exhaust nozzle.
3. Constriction of the exit area due to boundary layer build-up.
4. Jet detachment.
5. The gas velocity, pressure, temperature, and density are not uniform across any section normal to the nozzle axis.
6. The propellant is not a true perfect gas and is not homogeneous and invariant within the chamber and nozzle.[2]

The last condition allows the implementation of the perfect gas law.

(1) $$p_x = \rho_x R T_x / M$$

where p, ρ, and T are the pressure, density, and temperature, respectively, at some point x, R is the universal gas constant (8314.3 Joule/k mol-°K), and M is the molecular mass of the propellant. For a perfect gas, the specific heat at

constant pressure, c_p, the specific heat at constant volume, c_v, and the ratio of the two are constant:

(2)
$$k = c_p/c_v$$

$$c_p - c_v = R/(MJ)$$

(3)
$$c_p = \frac{kR}{MJ(k-1)}$$

where J = 1 in SI units and 778 ft-lb/Btu in English units.

Applying the principle of conservation of energy in which the decrease in enthalpy is equal to the increase in kinetic energy of the propellant, we may write the enthalpy, which is the product of the specific heat and the absolute temperature, as:

(4)
$$h_1 - h_2 = c_p(T_1 - T_2) = (v_2^2 - v_1^2)/2J$$

where h is the enthalpy and v is the velocity at the chamber and the nozzle exit. Solving (4) for the nozzle exit velocity, v_2, yields:

(5)
$$v_2 = \sqrt{2J\,(h_1 - h_2) + v_1^2}$$

In addition, for isentropic flow, the following relations hold[2]:

(6)
$$T_1/T_2 = (p_1/p_2)^{(k-1)/k} = (\rho_2/\rho_1)^{k-1}$$

When the chamber cross section is large compared to the nozzle cross section, the chamber velocity, v_1, is small and may be neglected. Thus (5), (6), and (3) may be written as:

(7) $$\upsilon_2 = \sqrt{\frac{2kRT_1}{M(k-1)}\left[1 - \left(\frac{p_2}{p_1}\right)^{(k-1)/k}\right]}$$

Given the exit velocity it is now possible to determine the specific impulse, I_{sp}, of the fuel:

$$I_{sp} = F/(\dot{m}g_0)$$

where F is thrust, $\dot{m}$ is the mass flow rate of the propellant, and g_0 is standard sea-level gravity (9.80 m/s^2). The thrust may be defined as the integral of the pressure forces acting on the nozzle and chamber in the axial direction. This integral equates to:

$$F = \dot{m}\upsilon_2 + (p_2 - p_3)A_2$$

where the first term is known as the momentum thrust and the second as the pressure thrust. However, if the exit pressure is assumed to be equal to the ambient pressure, the pressure thrust term is zero and the specific impulse may be written as:

(8) $$I_{sp} = \upsilon_2/g_0$$

To determine the thrust, the mass flow rate is needed. The principle of conservation of matter is used and is expressed by equating the mass flow rates at any two sections:

(9) $$\dot{m}_1 = \dot{m}_2 = A_1\upsilon_1\rho_1 = A_2\upsilon_2\rho_2$$

Applying (6) and (7) to (9) yields the propellant mass flow rate in any section as a function of the chamber temperature and pressure ratio:

$$(10) \quad \dot{m}_x = \frac{A_x p_1 M\sqrt{2J}}{R} \sqrt{\left\{ \frac{c_p}{T_1} \left[\left(\frac{p_x}{p_1} \right)^{2/k} - \left(\frac{p_x}{p_1} \right)^{(k+1)/k} \right] \right\}}$$

The maximum propellant flow per unit area occurs at the throat, so the throat pressure, p_t, may be found by differentiating (10) with respect to x and setting the derivative to zero:

$$(11) \qquad \frac{p_t}{p_1} = \left(\frac{2}{k+1} \right)^{k/(k-1)}$$

From (11) it is now possible to determine the conditions for which subsonic, sonic, and supersonic flow at the throat occur. Referring to Figure 1, sonic or supersonic conditions at the throat occur if the chamber to exit pressure ratio (p_1/p_2) is equal to or greater than p_t/p_1. Subsonic throat conditions occur if p_1/p_2 is less than p_t/p_1. In addition, chamber pressures below a given level will also result in subsonic flow. This level is approximately 2.17 atm for nitrogen and 2.6 for ammonia when operating at sea-level. Typically, the supersonic nozzle is used for rocket engines because the lower velocities associated with subsonic flow tend to lower the specific impulse below practical levels for space flight.

Continuing our determination of the rocket thrust, we combine (11) with the isentropic relationships in (6) to determine the density and temperature at the throat:

$$(12) \qquad \rho_t = \rho_1 \left(\frac{2}{k+1} \right)^{1/(k-1)}$$

and

(13) $$T_t = \frac{2T_1}{k+1}$$

and combining (7), (11), and (13) results in the throat velocity equation:

(14) $$v_t = \sqrt{\frac{2kRT_1}{M(k+1)}}$$

Thus we may now write the mass flow rate for a supersonic nozzle as a function of those variables which are design controlled: throat area, chamber pressure, chamber temperature, and specific heat ratio:

(15) $$\dot{m} = A_t p_1 k \sqrt{\frac{\left(2/(k+1)\right)^{(k+1)/(k-1)}}{kRT_1}}$$

Likewise, using the *perfect* gas law, and equations (7), (12), and (14), it is possible to relate another important design parameter, the expansion or area ratio, A_2/A_t, to the pressure ratio p_2/p_1:

(16) $$\frac{A_t}{A_2} = \left(\frac{k+1}{2}\right)^{1/(k-1)} \left(\frac{p_2}{p_1}\right)^{1/k} \sqrt{\frac{k+1}{k-1}\left[1 - \left(\frac{p_2}{p_1}\right)^{k-1/k}\right]}$$

Also, given the expansion ratio, the throat area, and the divergence angle of the nozzle, α, the nozzle length may be derived from simple geometry:

(17) $$L = \sqrt{\frac{A_t}{\pi \tan^2(\alpha)}} \left(\sqrt{\frac{A_2}{A_t}} - 1 \right)$$

Finally, we are in a position to relate the thrust of a supersonic nozzle to the design parameters. Given that the thrust, defined earlier, may be written as:

$$F = \dot{m}v_2 + (p_2 - p_3)A_2$$

Note that in orbit the external pressure p_3 is negligible, the thrust equation above simplifies to:

$$F = \dot{m}v_2 + p_2A_2$$

It is also interesting to note that the maximum thrust occurs when p_2 is zero, causing v_2 to be maximized. Once again by combining equations (7), (12), and (14) we may relate the thrust to the design parameters A_t, p_1, k, and A_2/A_t (which gives p_2/p_1) in a form known as the ideal thrust equation:

$$(18) \qquad F = A_t p_1 \sqrt{\frac{2k^2}{k-1}\left(\frac{2}{k+1}\right)^{\frac{(k+1)}{(k-1)}}\left[1 - \left(\frac{p_2}{p_1}\right)^{(k-1)/k}\right]} + A_2 p_2$$

Another form of the ideal thrust equation normalizes the force by dividing (18) by the throat area and chamber pressure, thus the unitless variable F/A_tP_1 becomes a function of the area ratio A_2/A_t and the pressure ratio p_2/p_1 only.

Validation Case

To evaluate the above equations, data from a cold gas ammonia propulsion system designed for the Lincoln Experimental Satellites LES-8 and LES-9 were used.[3] The propulsion system for both satellites was provided by TRW Systems Group under contract to M.I.T. Lincoln Laboratory. Both have identical, cold ammonia propulsion systems with a specific impulse of 100 seconds operating in a design range of -10°C to 40°C. Given the 15° divergence angle and an expansion ratio of 60:1, a nozzle length of 0.746 cm may be calculated. Finally, with a 1.55×10^{-7} m^2 throat area and a chamber pressure of about 0.207 MPa, thrust levels of 0.045 N were achieved.

Applying this data to the equation presented earlier, it is possible to construct a plot of I_{sp} versus area ratio as shown in Figure 2 and to confirm an I_{sp} of 100 seconds for an area ratio of 60:1. Likewise, Figure 3 illustrates a plot of equation (16) from which one may determine that the pressure ratios produced from a 60:1 area ratio at chamber temperatures of -10°C and 40°C are about 950 and 1725, respectively. These ratios represent the minimum and maximum pressure ratios obtainable for an ammonia system having the given expansion ratio operating over the given temperature range. Finally, the thrust is obtained from equation (18). Here we see the theoretical thrust levels obtainable from a supersonic nozzle with a throat area of 1.55×10^{-7} m^2, a 60:1 expansion ratio, a chamber pressure of 0.207 MPa, and pressure ratios of 950 to 1725 are 0.056 to 0.060 Newtons.

The disparity between the calculated thrusts and the Lincoln measured thrust of 0.045 Newtons is a result of the ideal nozzle assumptions made earlier. The first of these accounts for conical divergence of the exhaust jet. In comparison to the ideal nozzle flow, which assumes axially aligned flow, the

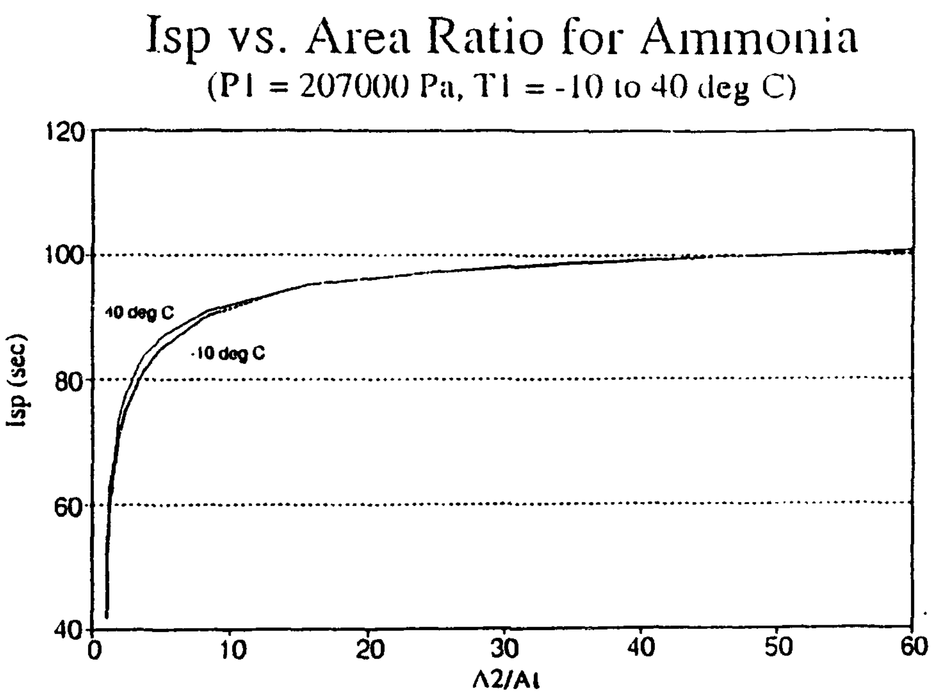

Figure 2

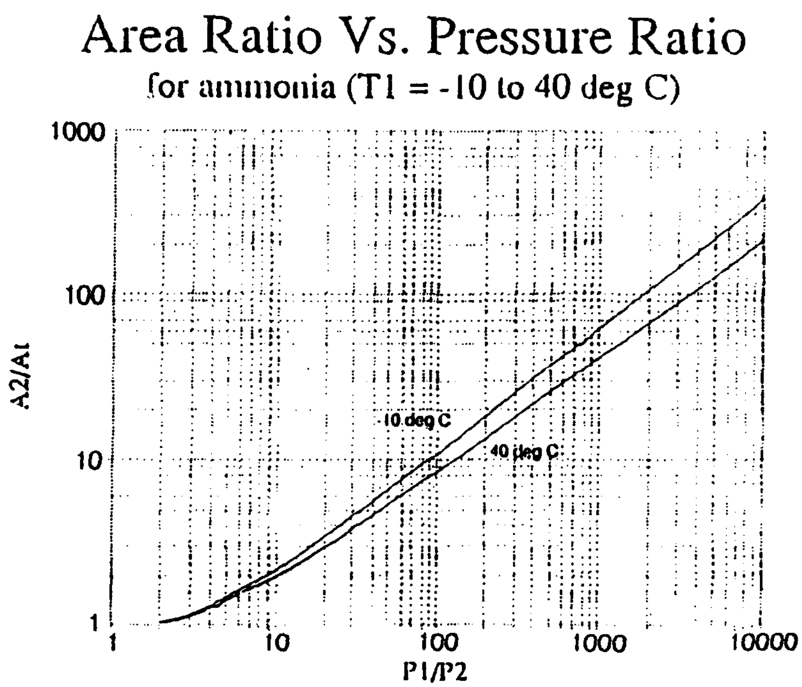

Figure 3

real rocket contains some element of non axially directed flow which results in a thrust loss. This loss, given in Altman, may be simplified to:

$$F = F_0(1 + \cos \alpha) / 2$$

where F_0 is the ideal thrust, and α is the divergence angle. Thus for an α of 20^0, the thrust due to conical divergence is about 97% of the ideal thrust. Table 1 lists the thrust correction factor due to various divergence angles.

Divergence Angle (deg)	Thrust Correction Factor
0	1.0000
10	0.9924
20	0.9698
30	0.9330

Table 1: Thrust Correction Factors for Various Divergence Angles[2]

The second ideal rocket assumption neglected surface friction and flow disturbances. Losses due to these effects are difficult to calculate, however, they may be minimized by reducing sharp curves at the throat. Typical losses due to friction flow are about 1 to 3%.

The third assumption neglected constriction of the exit area due to boundary layer effects. These effects are most prominent at the nozzle exit and have the effect of reducing the operating expansion ratio. According to Altman, observations of boundary layer growth in the Reynolds number region from 5×10^5 to 5×10^6 and a Mach number range of 1.5 to 2.5 produce the following approximate relationship between boundary layer displacement thickness, d,

and nozzle length, L:

$$d = 0.004L$$

Applying this equation and (17) to the Lincoln example, the nozzle length is 0.0041 m, assuming a divergence angle of 20^{o}, and the boundary layer displacement is 1.65×10^{-6} m. Simple geometry reveals that the expansion ratio has been reduced from 60:1 to 59.856:1. However, this reduction in expansion ratio only produces a thrust loss of 0.005%.

Likewise, the remaining assumptions have negligible effects on the thrust output and are difficult to calculate outside of experimentation. According to Altman, the combined thrust loss due to these assumptions is less than 5%.

Having applied these corrections to the calculated thrust, a 15 to 20% difference still exists between the calculated and measured thrust reported for the LES system. This difference is unaccounted for but may be due to errors in the measured thrust data, calculated data, or the interpretation of the LES system design.

Design Process

For the Shuttle, the accelerations due to gravity and drag are the primary disturbances in the low frequency (< 0.1 Hz) range. These forces may vary from 0 to 5 Newtons, depending on the Shuttle angle of attack. In order to counter these forces, a 0 to 2 Newton microthruster using gaseous Nitrogen as the cold gas propellant has been designed. Four of these thrusters strategically placed within the cargo bay may then be used to create a microgravity environment of 10^{-6} G or smaller for a position off-set from the Shuttle center of gravity.

Nitrogen was the gas of choice due to its low molecular weight and density. This allows for high specific impulses and the ability to store more propellant. Originally a two-phase system was considered because of its increased propellant storage capability, however system complexity and difficulties involved in phase separation soon outweighed this benefit.

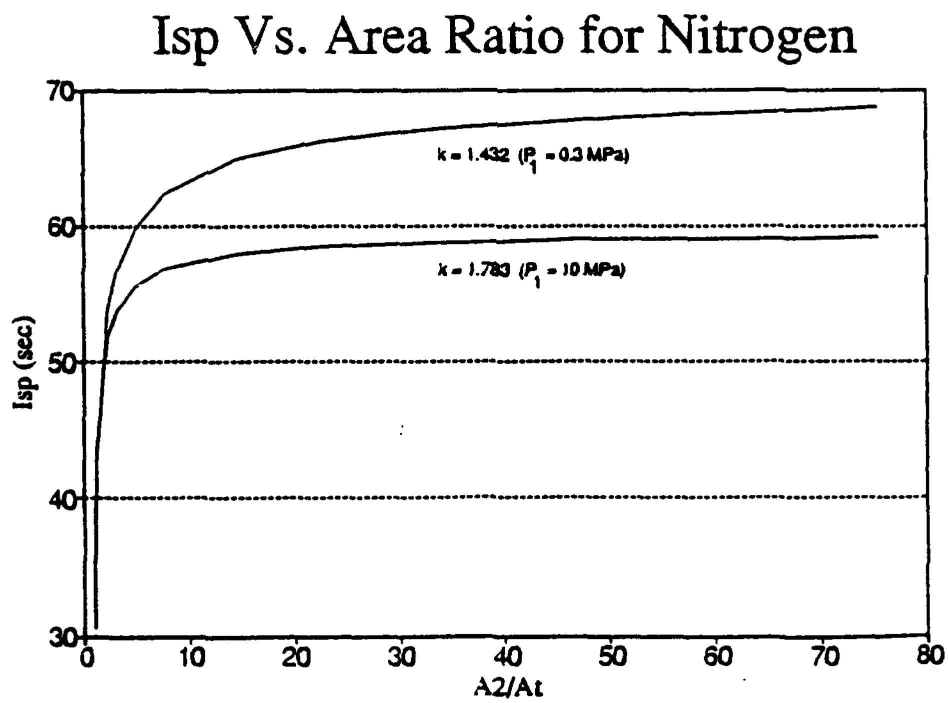

Figure 4

Using gaseous nitrogen, and assuming an average cargo bay temperature (chamber temperature) of -20°C and a chamber pressure range of 0.3 to 10 MPa, a range of k values from 1.432 to 1.783 may be obtained from chemical properties tables. The pressures used roughly correspond to the minimum pressure allowable for supersonic flow, and 25% of the maximum pressure obtainable from a flight qualified cold gas storage tank (3000-5000 psi). The 25% was chosen as being the lowest storage pressure allowable to maintain the desired thrust levels.

Assuming that throat areas below 1 x 10^{-7} m^2 require the use of fuel filters, and that excessive nozzle size and mass will not be inhibitory, we are left only to decide the expansion ratio, throat area, and length of that will produce 0 to 2 Newtons of thrust for the given pressure range.

In order to maximize the specific impulse of nitrogen, the I_{sp} versus area ratio has been plotted in Figure 4. From this figure we see that an expansion ratio of about 8:1 will yield 95% of the theoretical maximum I_{sp} for a k value of 1.783, while a ratio of about 64:1 will yield 95% of the maximum I_{sp} for a k of 1.432. As a result, an expansion ratio of 64:1 will maximize I_{sp} efficiency for either value of k.

Given an expansion ratio of 64:1, equation (16) may now be used to determine the resulting pressure ratio (p_1/p_2) associated with that area ratio. Figure 5 shows the relation between the two ratios and reveals that for a 64:1 expansion ratio, a pressure ratio of 2355 will be achieved.

Finally, knowing the desired thrust range and the given pressure range, it is possible to use equation (18) to plot the thrust versus chamber pressure for various throat areas, as seen in Figure 6. This plot assumes that the value of k varies linearly from 1.432 to 1.783 as the pressure increases from 0.3 to 10 MPa. From Figure 6, we see that a throat area of 1 x 10^{-7} m^2 will produce thrust

from 0.08 to 1.58 N while a throat area of 1.25 x 10^{-7} m^2 will produce a thrust of 0.10 to 1.99 N, thus the thrust range for either design is about the same. These particular values were chosen because they come closest to meeting the 0 to 2 N design requirement, although the throat area will most likely be set by the maximum required thrust, not the minimum required thrust.

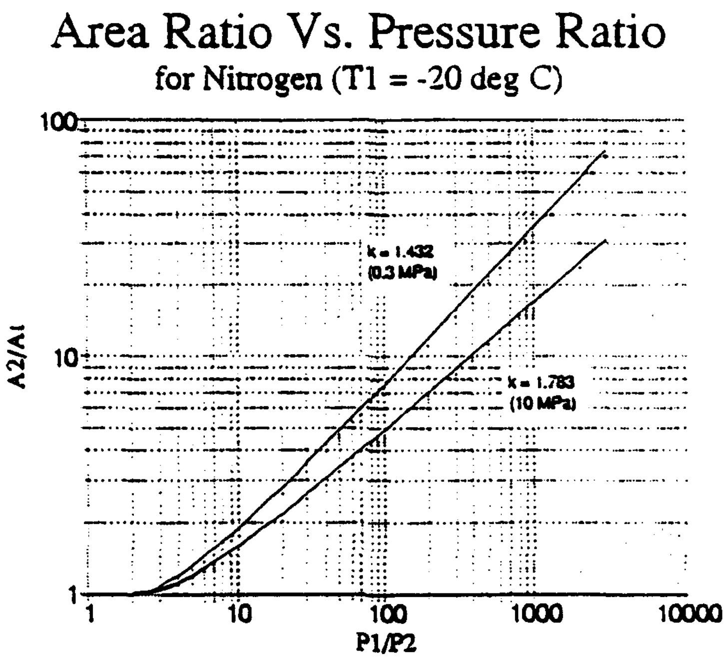

Figure 5

Determining the length associated with this nozzle requires the use of equation (17). For the 1.25 x 10^{-7} m^2 throat area and a divergence angle of 20°, the length is 3.08 cm, while a divergence angle of 5° yields a length of 12.81 cm. For such a disparity in length, one needs to decide if the thrust losses associated with a 20° divergence angle is worth the reduction in length. From Table 1 we see a thrust loss of 3% for the 20° angle and 1% for the 5° angle, both within the error range for the ideal nozzle assumptions. However, the fragility of the nozzle and the possibility of damage are probably much higher for a 21 cm nozzle, thus a higher divergence angle is recommended.

In conclusion, Table 2 summarizes the microthruster design.

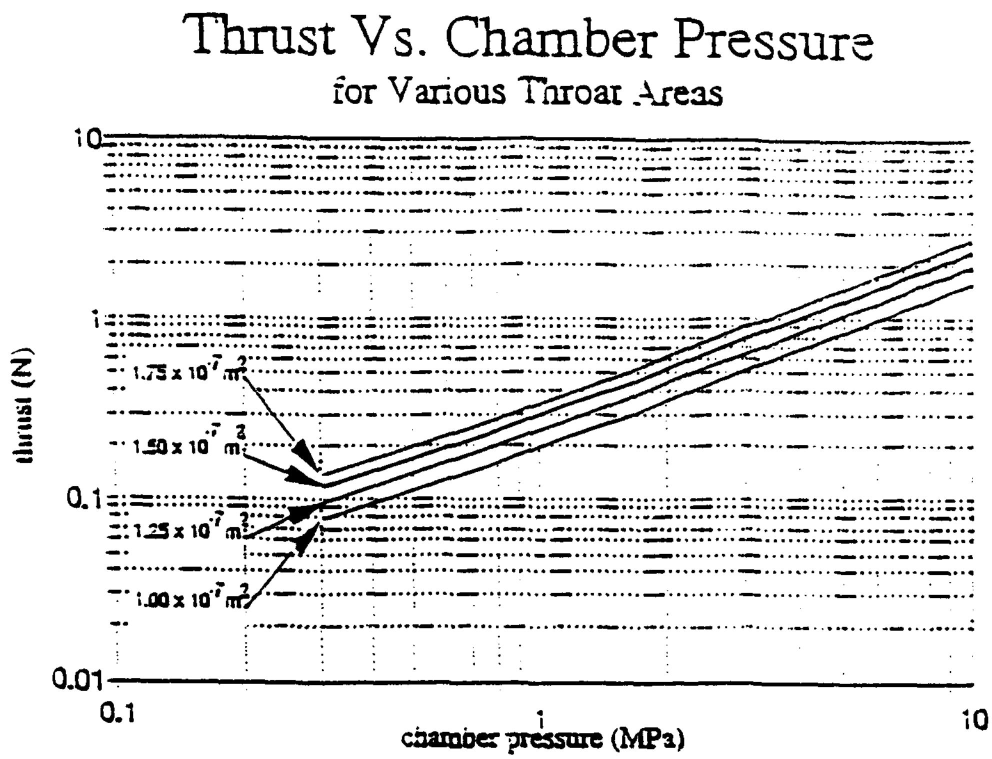

Figure 6

Propellant	Gaseous Nitrogen
Specific Impulse	72 sec
Expansion Ratio	64:1
Throat Area	1.25×10^{-7} m^2
Chamber Pressure	0.3 to 10 MPa
Chamber Temperature	-20° C
Length	3.08 cm
Divergence Angle	20°
Thrust	0.1 to 2 N
Mass Flow Rate	3.4 to 0.1 g/sec

Table 2: Microthruster Design Parameters

References

1. Altman, David, et al. Liquid Propellant Rockets. Princeton University Press, Princeton, 1960, Pp 122-130.

2. Sutton, George P. Rocket Propulsion Elements. 5th ed. Wiley & Sons, New York, 1986. Pp 35-49.

3. Murch, C.K. and F.W. Floyd, Jr. "The Cold Ammonia Propulsion System for the Lincoln Experimental Satellites LES-8 and -9." TRW Systems Group, Redondo Beach, Ca.

MISSION ANALYSIS

FOR

SMALL ELV-BASED, IN-SPACE OPERATIONS

Davy A. Haynes,
Scott Baune,
John Lussier &
Mike Rice

Space Technology Initiative Ofice
NASA Langley Research Center

SELV-Based In-Space Operations Workshop
Newport News, Virginia
October 18-19, 1993

Mission Analysis Overview

- Survey of Candidate Missions
- Definition of Mission Categories and Types
- Mission Type Characterization
- Preliminary Mission Analysis
- Conclusions and Recommendations

Survey of Candidate Missions

Palapa B2

Type: Communications

Owner: Perumtel (Indonesia)

Manufacturer: Hughes

Launched: 4 Feb 84 (Shuttle)

Mass: 1240 kg at launch, 652 kg on station @ BOL

Orbit: 108 deg E Geostationary

Design Life: 8 years

Failure: Initially stranded in 237 X 1046 km orbit after failure of PAM-D GTO insertion stage. Moved to 1207 km orbit then lowered to Shuttle altitude using all reserve propellant. Recovered by Shuttle in Nov 84 and sold to Sattel Technologies for $18-21 M. Re-launched Apr 85 after a $7 M refurbishment by Hughes. Resold to Indonesia for $137.5 M.

Mission Classification: Reboost of valuable asset in improper orbit.

Survey of Candidate Missions

Westar VI

Type: Communications

Owner: Western Union

Manufacturer: Hughes

Launched: 4 Feb 84 (Shuttle)

Mass: 1100 kg at launch, 582 kg on-station @ BOL

Orbit: Geostationary

Design Life: 10 years

Failure: Stranded in 266 X 1059 km orbit after failure of PAM-D GTO insertion stage. Boosted to 1060 X 1066 km by the AKM to prevent atomic oxygen damage, then lowered to Shuttle altitude for retrieval. Later refurbished and relaunched as AsiaSat 1 by Asia Satellite.

Mission Classification: Reboost of valuable asset in improper orbit.

Survey of Candidate Missions

Superbird A

Type: Communications

Owner: Space Communications Corp. of Japan

Manufacturer: Ford Aerospace (SS/Loral)

Launched: 5 Jun 89 (Ariane IV)

Mass: 2492 kg at launch, 1505 kg on-station @ BOL

Orbit: 158 deg E geostationary

Design Life: 10 years

Failure: Lost most of its station keeping oxidizer on Dec 90 possibly due to a command error. Commercial operations ended and $170 M in insurance was paid.

Mission Classification: Refuel (oxidizer) of otherwise fully-functional valuable asset.

Survey of Candidate Missions

INSAT 1A

Type: Communications

Owner: Indian National Satellite Systems

Manufacturer: Ford Aerospace (SS/Loral)

Launched: Apr 82 (Delta)

Mass: 1152 kg at launch, 650 kg on-station @ BOL

Orbit: Geostationary

Design Life: 7 years

Failure: Abandoned after 5 months when attitude control propellant was exhausted. $70 M insurance was paid.

Mission Classification: Refuel of otherwise fully-functional geostationary satellite.

Survey of Candidate Missions

INSAT 1C

Type: Communications

Owner: Indian National Satellite Systems

Manufacturer: Ford Aerospace (SS/Loral)

Launched: 21 Jul 88 (Ariane)

Mass: 1152 kg at launch, 650 kg on-station @ BOL

Orbit: 93.5 deg E Geostationary

Design Life: 7 years

Failure: Power system failure due to a isolation diode short on a solar panel. Communications lock was lost Nov 88 and the spacecraft was abandoned, resulting in an insurance payoff of $70 M.

Mission Classification: Repair (solar panel replacement) of asset in geostationary orbit. Functional status unknown.

Survey of Candidate Missions

ARABSAT 1A

Type: Communications

Owner: ASCO/Saudi Arabia

Manufacturer: Space Systems-Loral

Launched: 8 Feb 85 (Ariane)

Mass: 592 kg on-station @ BOL

Orbit: 19 deg E Geostationary

Design Life: 7 years

Failure: About one month after launch, power to two ACS gyros failed causing North-South station keeping to be exercised manually. The spacecraft, although partially functional, was declared an in-orbit spare and $75 M insurance was paid.

Mission Classification: Repair (power distribution) of a partially functional asset.

Survey of Candidate Missions

et al

Hipparcos (Aug 89): ESA science spacecraft stranded by booster failure.

STTW-T1 (Jan 84): Chinese communications satellite stranded by booster failure.

Telecom 1B (May 85): French communications satellite drifted from GEO due to RCS failure.

TDF-1 (Oct 88): French communications satellite loses transponder due to electrical arcing via a propellant leak.

TDF-2 (Jul 90): French communications satellite losses two traveling wave tube amplifiers when inadvertently shutdown by a safety mechanism.

TV-Sat 1 (Nov 87): German communications satellite suffered from failed deployment of a solar panel.

BS-2 (Jan 84): Japanese communications satellite suffered from loss of two out of three transponders.

BS-3 (Aug 90): Japanese communications satellite suffered from failure of one out of four solar panels.

Definition of Mission Categories and Types

Reboost

Definition

Propulsively reposition a satellite into a new orbit.

Subcategories

LEO Reboost: raise a spacecraft's orbit to compensate for and prevent orbital decay.

GTO Insertion: perform GTO insertion for stranded GEO satellite. Might also have to perform subsequent apogee (circularization and inclination change) maneuver.

Definition of Mission Categories and Types

Retrieval

Definition

Safely return a spacecraft to Earth for repair, refurbishment, salvage, or study.

Subcategories

Direct Recovery

Recovery via STS: lower a spacecraft to an altitude that is accessible by the Shuttle.

Definition of Mission Categories and Types

Deorbit/Disposal

Definition

Perform a propulsive maneuver to deorbit or dispose of a satellite which is no longer needed or functional.

Subcategories

Deorbit: Propulsive maneuver is such that the satellite is destroyed upon reentry over an unpopulated area. *Primarily for LEO spacecraft.*

Disposal: Propulsive maneuver is such that the satellite is moved to a safe orbit for deactivation. *Primarily for GEO spacecraft.*

Definition of Mission Categories and Types

Refuel

<u>Definition</u>

Replenish a satellite's supply of fluid consumables by refilling the S/C's propellant/pressurant tanks, or by supplemental tanks.

<u>Subcategories</u>

RCS fuel/oxidizer: resupply fuel and/or oxidizer for the S/C's reaction control system.

Pressurant: resupply pressurant gases (N2, He, etc.) used to pressurize S/C propellant tanks.

Definition of Mission Categories and Types

Repair

Definition

Overcoming a dysfunctional component, system, or spacecraft to attain a fully-function spacecraft; or to significantly improve the spacecrafts functional status.

Subcategories

Restoration: to return the dysfunction system to service by repairing (fixing) the failure.

Replacement: to physically replace the dysfunction component with a new unit.

Supplement: to bypass the dysfunctional component by supplying a new unit to provide the function without physical replacement.

Definition of Mission Categories and Types

Payload Delivery/Recovery

Definition

Deliver and/or recover specialized payloads to assets already in orbit.

Subcategories

Critical hardware delivery (Space Station).

Critical crew recovery vehicle (Space Station).

Mission Type Characterization

Candidate missions were separated into LEO, MEO, and GEO to allow a characterization of mission types based upon SELV performance.

LEO includes spacecraft at altitudes up to 800 km at any orbital inclination.

- HST (Hubble Space Telescope)
- EOS (Earth Observing System) satellites
- SSF (Space Station Freedom)
- Nimbus weather satellites

MEO includes satellites at altitudes up to 10,000 km at any orbital inclination.

- GPS (global positioning system) satellites

GEO includes all geostationary satellites--36,000 km equatorial.

- Nearly all communications satellites

Mission Type Characterization

Available SELV's, with reasonalble assumptions for growth, bound the performance envelope of interest.

- Pegasus/Taurus (Orbital Sciences)
- MSLS (Martin Marietta)
- Conestoga (EER Systems)
- LLV1 (Lockeed)
- ORBEX (CTA)

Guidelines [performance] for the subsequent analysis.

- LEO (<800 km): not more than 2,000 kg
- MEO (800-10,000 km): 500-1,000 kg
- GTO (36,000 km apogee): not more than 500 kg

Note that all missions assume an automated rendezvous and docking capability.

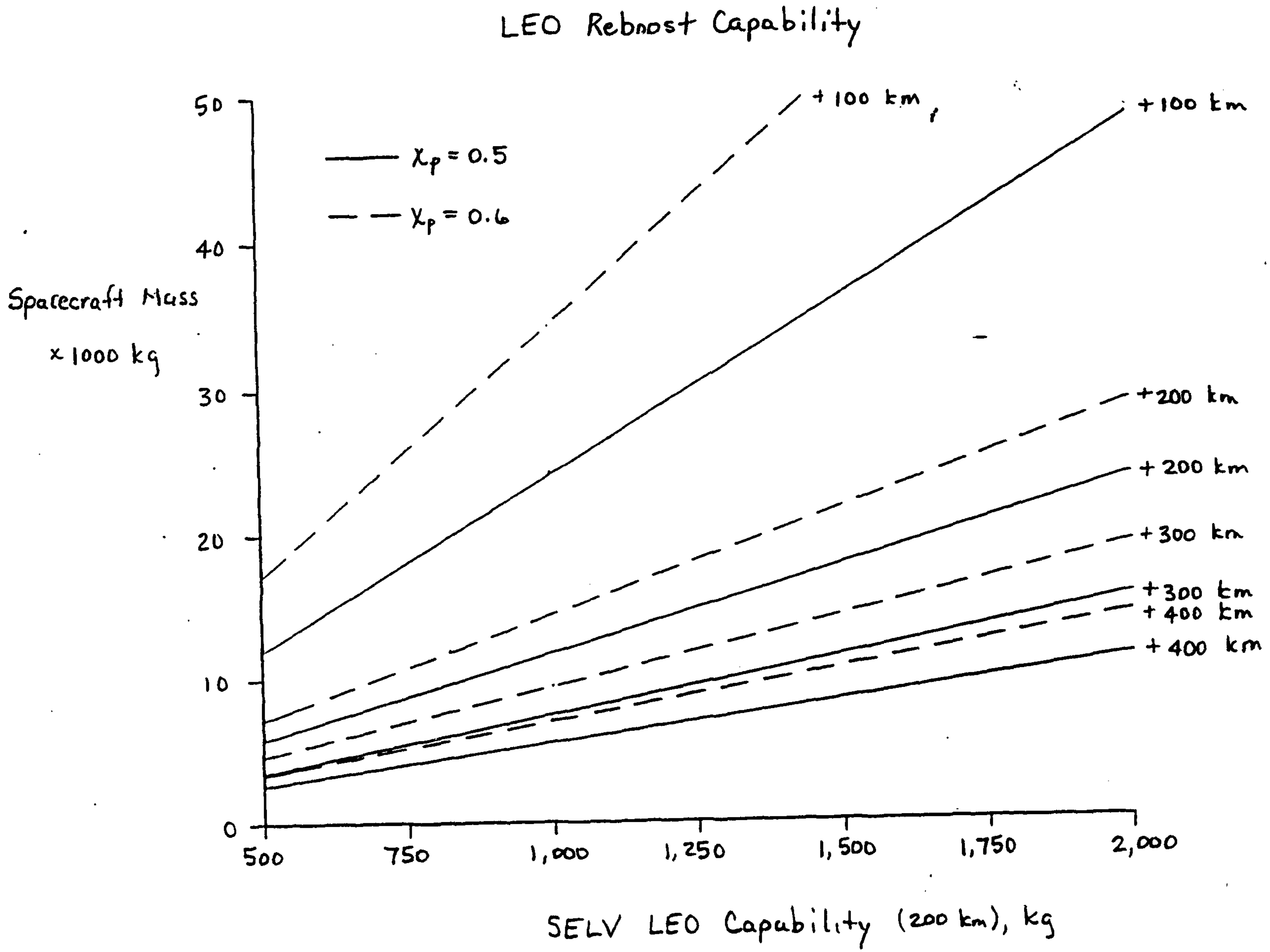

LEO Rebnost Capability
$\chi_p = 0.5$
$\chi_p = 0.6$
+100 km
+100 km
+200 km
+200 km
+300 km
+300 km
+400 km
+400 km
Spacecraft Mass
x 1000 kg
0
10
20
30
40
50
500
750
1,000
1,250
1,500
1,750
2,000
SELV LEO Capability (200 km), kg

GTO Insertion Capability

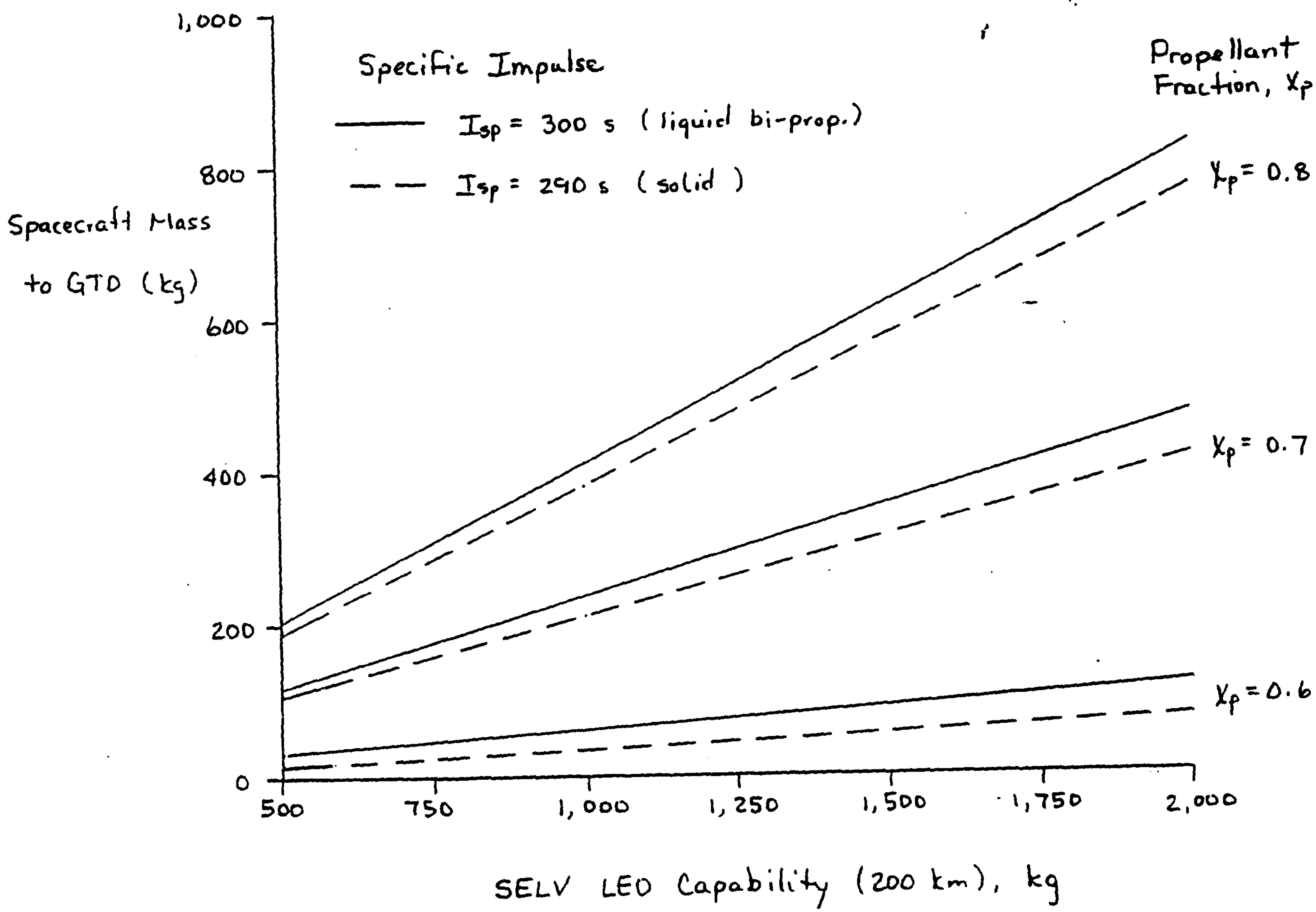

GEO Capability

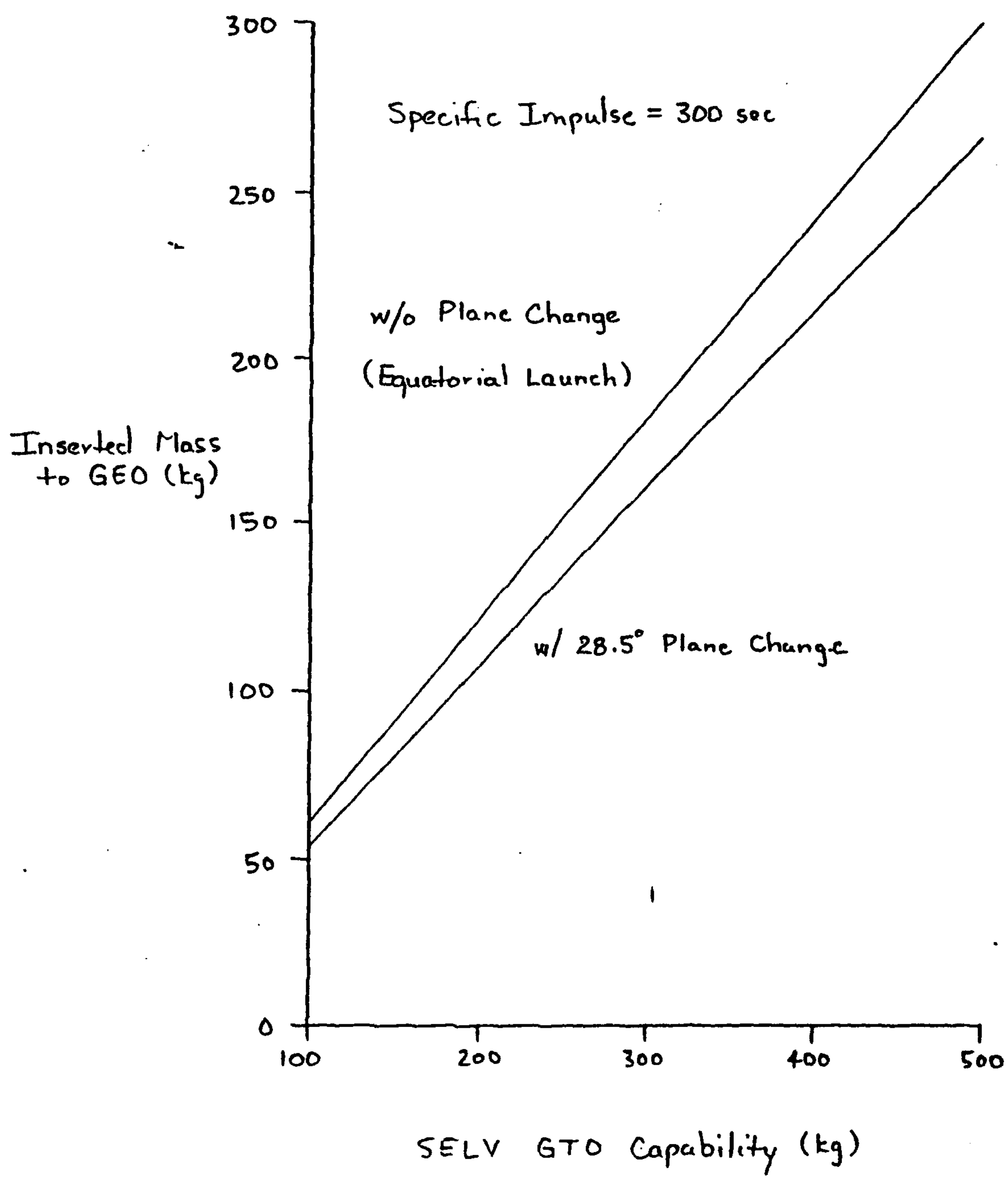

Propulsive Requirements for Satellite Disposal from GEO

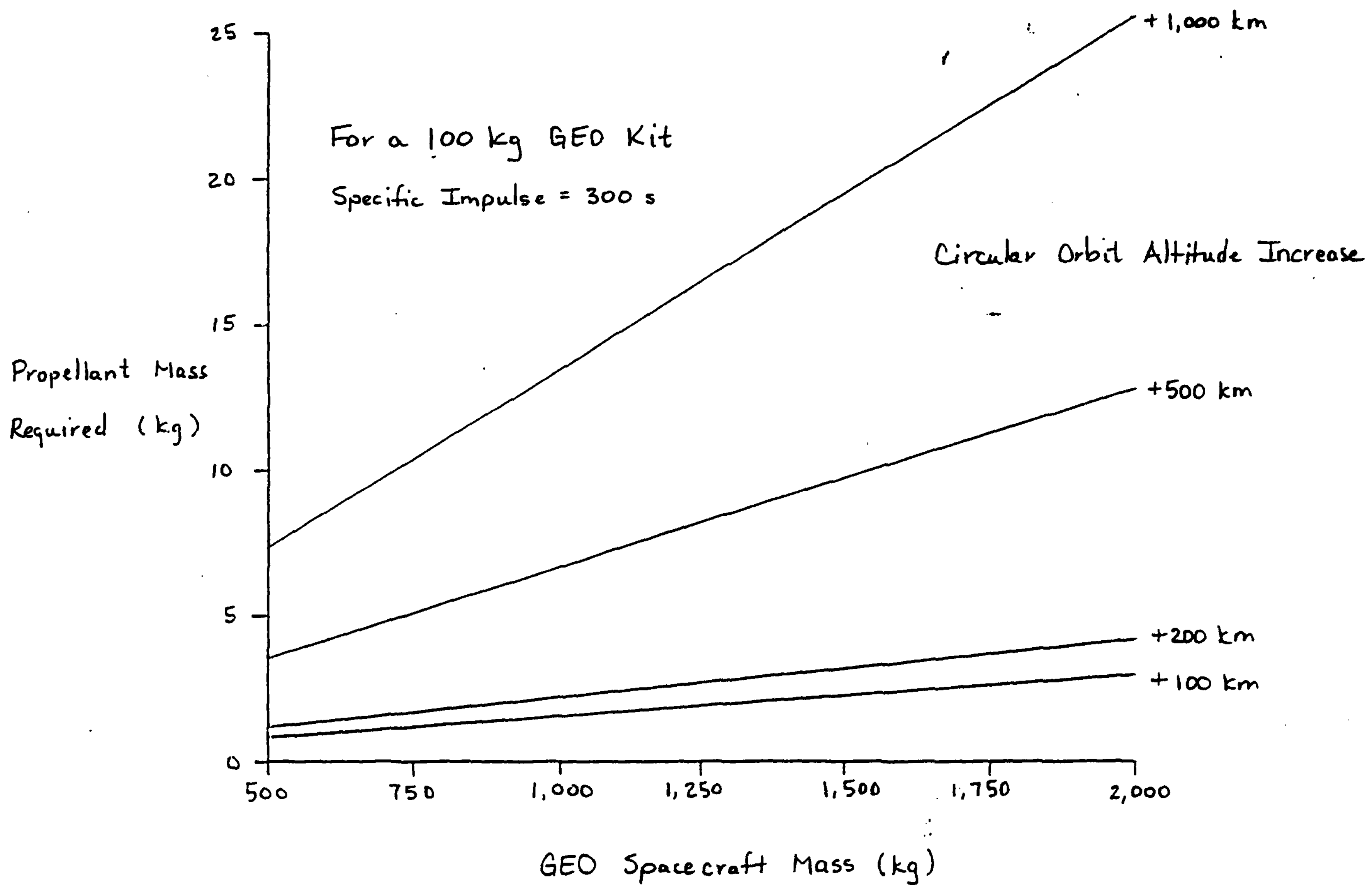

Preliminary Mission Analysis

Approach and Assumptions

Conceptualized various front-end spacecraft "kits" which would be tailored to suit the different mission categories.

Spacecraft kits would be ship-and-shoot, to minimize ground operations and preparation time.

Buses for the spacecraft kits would be short-lived (in orbit) to minimize development and testing.

Propulsion systems would be based on either solids or storable liquids and restricted to motors and engines already available.

Preliminary analysis aimed at eliminating those missions which would be improbable from a performance standpoint; and to shed insight on those missions feasible from a performance standpoint.

Analysis used to identify potentially attractive categories for subsequent conceptual mission design and analysis.

Preliminary Mission Analysis

Reboost--*Stranded Satellite Rescue*

Assuming a SELV places a propulsion "kit" in LEO, what is the bound on the mass of a spacecraft that it could dock with and insert into a GTO?

- Satellite initially stranded in a 200 km circular orbit.
- Propulsion system specific impulse (Isp) limited to about 290 s for solids, 300 s for available small storable liquids.
- Propellant mass fractions (of total kit mass) between 60-80%
- Satellite inserted into GTO only--would have to utilize its own AKM or on-board RCS for circularization maneuver.
- The low insertion masses, taken with the need for the satellite to perform its own circ maneuver, make reboost of communications satellites unlikely.
- However, LEO reboost (and MEO) is easily doable.

Preliminary Mission Analysis

Retrieval

Retrieval, or salvage of high-value spacecraft at the lower end of the SELV cost spectrum. Unfortunately, direct retrieval by an SELV-launched kit is not feasible for most satellites due to their size and mass.

- Retrieved satellite must be protected from reentry heating, aeroloads, and g-loads.

- Must be soft-landed by some means.

- An alternative for high-value payloads would be to use the kit to lower satellites to a Shuttle-accessible orbit for pick-up as a targets of opportunity.

Preliminary Mission Analysis

Deorbit

Deorbit of satellites in LEO is easily achievable for even very large satellites due to the low energy requirements for this type of mission.

Disposal

Disposal of GEO satellites may be accomplished by moving the unwanted satellite to a slightly higher orbit with small, two-burn propulsive maneuvers.

- The residual propulsive capability after a kit reaches GEO is extremely limited, especially for the larger comm. satellites.
- Fortunately, the propulsive requirements are small at this distance--even to move a satellite out 1,000 km.
- Similar to a refueling mission except that the kit would use its residual propellant.

Preliminary Mission Analysis

Refuel--*Replenish RCS Propellant*

Replenishing a satellite's consumables at GEO appears to be possible, particularly it the kit's own tanks are used.

- Mass of propellant required by most GEO satellites for station keeping is on the order of 10's of kg for several years of operation.

- Most GEO satellites utilize bi-prop thrusters which are compatible with the propellant of the kit itself.

- Dedicated tanks for the refuel propellants would not be required; thus increasing the "payload" margin.

- Since a refuel kit for GEO must be able to perform its own circ and rendezvous maneuvers, the same bus would easily be able to reach any LEO/MEO satellite.

- LEO, MEO, and GEO satellites all share similar station keeping propellant needs.

Preliminary Mission Analysis

Repair--*Fix, Replace, or Supplement*

Assuming a SELV places a repair "kit" into a GTO by direct injection, how much mass can be placed into GEO?

- Propulsion system based upon small liquid bi-props with a 300 s specific impulse.
- Overall kit mass is too small to make realistic estimates of what payload fractions might be.
- SELV insertion accuracies may make rendezvous at GEO complex and expensive.
- The good news is that SELV launch from near the equator can increase payloads to GEO by about 20%.
- Usable payloads to GEO will be small (10's of kg).
- Usable payloads to MEO will be on the order of 100 kg.
- Usable payloads to LEO can be nearly 1,000 kg.

Preliminary Mission Analysis

Delivery/Recovery

The only identified mission is Space Station logistics--in particular delivery of critical items needed for repairs that cannot wait for a Shuttle flight that may be several months away.

- An air-launched SELV, such as Pegasus, has the added advantage that orbital plane alignment can be obtained using the carrier aircraft--large launch windows.

- Recovery of payloads from the Space Station would also be possible, but is a much bigger problem.

- Perhaps a better use of a delivery kit, after it has performed its initial mission, would be to dispose of Space Station refuse by reentry incineration.

Preliminary Mission Analysis

Mission Matrix	LEO	MEO	GEO
Repair - Restore - Replace - Supplement	YES (T)	YES (T)	POSSIBLY (T&P)
Refuel	YES	YES	YES (P)
Deorbit/Disposal	YES	NEED?	YES
Delivery/Recovery	YES (SSF)	N/A	N/A
Retrieve - Direct - via STS	SOME (P)	NO (P)	NO (P)
Reboost	YES	YES (P)	UNLIKELY (P)

Limiting Factors: P=performance, T=technology

Conclusions and Recommendations

For LEO missions, current SELV performance is sufficient for all of the mission types with the exception of retrieval--although indirect retrieval via the Shuttle is still a possibility.

For MEO missions, current SELV performance is sufficient for repair, refuel, and boost (for MEO satellites stranded in LEO by booster failure).

For GEO missions, the SELV top performers have performance approaching what is needed to do low-mass repair, refuel, and disposal missions.

Reboost of GEO satellites stranded in low orbits is possible, but only for smaller satellites which posses their own apogee kick maneuver capability.

Launching GEO missions from equitorial locations can provide about a 20% performance increase.

Conclusions and Recommendations

Mission Matrix	LEO	MEO	GEO
Repair - Restore - Replac - Supple ent	YES (T)	YES (T)	POSSIBLY (T&P)
Refuel	YES	YES	YES (P)
Deorbit/Disposal	YES	NEED?	YES
Delivery/Recovery	YES (SSF)	N/A	N/A
Retrieve - Direct - via STS	SOME (P)	NO (P)	NO (P)
Reboost	YES	YES (P)	UNLIKELY (P)

Limiting Factors: P=performance, T=technology